JAERI－M
4531

Measurement of the Plasma Current Distribution in a Tokamak Device with α-Particles Injected Transverse or Parallel to the Toroidal Axis

July 1971

S. Kawasaki* · K. Inoue · T. Takeda

M. Yoshikawa

日本原子力研究所
Japan Atomic Energy Research Institute

荷電粒子（α－粒子）入射によるプラズマ中の電流分布測定

日本原子力研究所東海研究所核融合研究室

川崎　温*・井上堅司・竹田辰興・吉川允二

（１９７１年７月受理）

要旨　　ＪＦＴ－２において，プラズマ柱を流れる電流の分布測定のための一方法として，荷電粒子（α－粒子）を入射することによりその軌道の偏移量からプラズマ中のポロイダル磁場の値を推定する方法を検討し，そのための予備的な推測をした。

偏移量はＪＦＴ－２のパラメータと通常入手し得るα－粒子源では充分大きく，測定にかかる。

粒子の軌道解析の外，測定の分解能，α－粒子源，検出器等についても簡単な討論が行なわれた。

＊　原研客員研究員，金沢大学理学部

JAERI-M 4531

Measurement of the Plasma Current Distribution in a Tokamak Device with α - Particles Injected Transverse or Parallel to the Toroidal Axis

S. KAWASAKI*, K. INOUE, T. TAKEDA and M. YOSHIKAWA
Thermonuclear Fusion Laboratory, Tokai, JAERI

(Received July 1971)

Abstract —— A method is proposed for measuring the current distribution in a Tokamak plasma column by injecting α - particles from a radioisotope. In this method, the plasma current distribution is determined by injecting the α - particles into a plasma column and analyzing their orbits with and without the plasma current.

In this report, the orbit analysis is presented for the axisymmetric linear geometry. The deviation calculated for the JFT-2 Tokamak parameters indicates that the present method is feasible.

The problems of measurement resolution, toroidal effect, α - source and detector are also described.

---

* Visitting Scientist on leave from Kanazawa University, Kanazawa, Japan.

目　次　な　し

1. Introduction

One of the most important measurements in a Tokamak experiment is that of the distribution of plasma current to analyse the equilibrium and stability of the plasma column. We have proposed a method for measuring the distribution by injecting neutral particles into the plasma and measuring their orbit after being ionized in the plasma.[1] The method has many advantages as follows: the energy of particles may be varied, so that the ion gyroradius fits the radius of the plasma column and the beam intensity required for the method is currently available and can be amplitude- modulated in order to improve the accuracy of the measurement. Further more, the neutral particles can be introduced into the device without special transport system such as the magnetic shield which may be required injecting of charged particles. On the contrary, the neutral beam source is rather expensive to build and more essentially, there is a complication that the ions may become not only singly ionized but also multiply ionized. The present condition makes it necessary to determine the deviation and angle of the orbit at the detector.

The situation could be improved by a use of a charged heavy particle radiated from a radio-isotope, such as α-particle from Po^{210} [2]. The radiation source is small enough to be placed near the plasma surface. The measurement of particle orbit with and without the plasma current make it possible to determine the distribution of plasma current in the plasma column.

Technical problems encountered are in the preparation of the source of suficiently high intensity and detector system. We will review here the study made so far on the possibility of measuring the current distribution by means of charged particle, especially α - particle.

2. Orbit Analysis of Charged Particles

2-1 Linear Geometry

At first, we limit ourselves to the problem of two dimensions, that is, without the toroidal effect and with the axial symmetry.

$$\left[\frac{2E}{m}-r^2\left\{\omega_0^2\left(1-\frac{r_0^2}{r^2}\right)-\dot{\theta}_0\frac{r_0^2}{r^2}\right\}^2-\left\{\frac{e}{m}\left(A_Z(r)-A_Z(r_0)\right)-\dot{Z}_0\right\}^2\right]$$

$$=0 \qquad (9)$$

From (4), (6) and (8) the orbit of the charged particles in the plasma and then its deviation from the orbit without the plasma current is calculated.

2-2 Plasma Current Distribution

Now we shall give an actual representation for $A_z(r)$ or the distribution of plasma current in the following two cases:

1.

$$j=j(r)=j_0\frac{n+2}{2}\left(\frac{r}{a}\right)^n \qquad n: \text{zero or positive integer.} \qquad (10)$$

where $j_0=I/\pi a^2$, I is the total plasma current and a is the radius of the plasma column. I and a are supposed to be constant. In this case the θ - component of the magnetic field produced by the plasma current, B_p and the vector potential $A_z(r)$ are

$$B_p=\mu_0\frac{j_0}{2a^n}r^{n+1} \qquad (11)$$

and

$$A_z(r)-A_z(r_0)=\frac{\mu_0 j_0}{2(n+2)a^n}\left(r_0^{n+2}-r^{n+2}\right) \qquad (12)$$

The current distributions for n = 0, 1, 2, ... are shown in Fig. 2.

2. $$j=j_0\frac{p+2}{p}\left[1-\left(\frac{r}{a}\right)^p\right] \qquad p: \text{positive integer} \qquad (13)$$

gives

$$B_p=\mu_0\frac{p+2}{p}j_0\left[\frac{r}{2}-\frac{r^{p+1}}{a^p(p+2)}\right] \qquad (14)$$

$$A_z(r)-A_z(r_0)=-\mu_0\frac{p+2}{p}j_0\left[\frac{r^2}{4}\Big|_{r_0}^{r}-\frac{r^{p+2}}{a^p(p+2)^2}\Big|_{r_0}^{r}\right] \qquad (15)$$

The distributions for p = 1, 2, ... are shown in Fig. 3.

It should be noted that (10) and (13) show the monotoneously increasing (or decreasing) distribution and any distribution can not be represented in these forms. The solutions of (4), (6) and (8) are generally given in the form of the super elliptic integrals and hardly treated with ease.

2-3 Small Deviation from the Motion in the Vacuum Field

In most cases B_p is much less than B_z applied externally and the perturbation method will be useful.

1. Zero order solution

From (8) with $j_0 = 0$ or $A_z - A_z(r_0) = 0$

$$\int_{r_0}^{r} \frac{dr}{\left[\frac{2E}{m} - \dot{Z}_0^2 - r^2\left\{\omega_0\left(1 - \frac{r_0^2}{r^2}\right) - \dot{\theta}_0 \frac{r^2}{r_0^2}\right\}^2\right]^{1/2}} = t \tag{16}$$

The projection of the orbit comes to be circle naturally. The particle source should be set outside but near the plasma column.

In order to get the knowledge of the distribution from the surface to the center of the plasma, the particle injected into the plasma must reach the center or the axis. If we suppose that $r_0 = a$ and $r_{min} = 0$, from (6)

$$\dot{\theta} = -\omega_0$$

and the radial position r is from (7) directly

$$r = r_0 \cos\omega_0 t + \frac{\dot{r}_0}{\omega_0} \sin\omega_0 t \tag{17}$$

for $\omega_0 > 0$, (17) may be zero order solution.

2. First order solution

We can put as

$$r = r_{(0)} + r_{(1)}$$

where

$$r_{(0)} = r_0 \cos\omega_0 t + \frac{\dot{r}_0}{\omega_0} \sin\omega_0 t \tag{18}$$

With (7) and (18),

$$2\dot{r}_{(1)}\dot{r}_{(0)} + \dot{r}_{(1)}^2 = -\frac{e^2}{m^2}\{A_z(r) - A_z(r_0)\}^2 + \frac{2e}{m}\{A_z(r) - A_z(r_0)\}\dot{Z}_0 \tag{19}$$

Neglecting the second term of the left side,

$$\dot{r}_{(1)} = \frac{1}{2\dot{r}_{(0)}}\left[-\frac{e^2}{m^2}\{A_z(r_{(0)})-A_z(r_0)\}^2 + \frac{2e}{m}\dot{Z}_0\{A_z(r_{(0)})-A_z(r_0)\}\right] \tag{20}$$

Considering the equation (3), the two cases will be treated:

(a) $\dot{z}_0 = 0$

where the deviation in the radial direction is of the second order and only that in the axial direction appears.

(b) $\dot{z}_0$ is comparable with $\sqrt{\frac{2E}{m}}$

where both of the deviations in the two directions come to appear.

2-4 Radial Drift

Cleary the radial deviation is given with non-zero initial axial velocity $\dot{z}_0$,

$$\dot{r}_{(1)} = \frac{1}{\dot{r}_{(0)}}\frac{e}{m}\dot{Z}_0\{A_z(r_{(0)})-A_z(r_0)\} = -\frac{e}{m}\int_{r_0}^{r}\dot{Z}_0 B_p \frac{dr_{(0)}}{dr_{(0)}/dt} = -\frac{e}{m}\dot{Z}_0\int_0^t B_p dt \tag{21}$$

(21) is a physically reasonable result. As shown in Fig. 4, the deviation of the velocity in the time interval in which the particle passes from r = 0 to r = a, $\Delta\dot{r}$ is

$$\Delta\dot{r} = -\frac{e}{m}\int_0^a \dot{Z}_0 B_p \frac{dr_{(0)}}{\dot{r}_{(0)}} \tag{22}$$

and equal to the deviation from r = a to r = 0

$$\Delta\dot{r} = -\frac{e}{m}\int_a^0 \dot{Z}_0 B_p \frac{dr_{(0)}}{\dot{r}_{(0)}} \tag{23}$$

, for $\dot{r}_{(0)}$ in (23) must take the polarity inverse to that in (22).

The less $\dot{r}_{(0)}$, the much $r_{(1)}$ can be obtained. The best solution is for $\dot{r}_0 = 0$ where the projected orbit of the particle into $r - \theta$ plane is contained within the plasma during one complete Larmor cycle. Zero order solution is

$$r = r_0 \cos\omega_0 t \quad (0 \leqq t \leqq \frac{\pi}{2\omega_0}) \tag{24}$$

$$\dot{r} = -r_0 \omega_0 \sin\omega_0 t$$

and

$$r = -r_0 \cos\omega_0 t \tag{25}$$

$$\dot{r} = r_0 \omega_0 \sin\omega_0 t \quad (\frac{\pi}{2\omega_0} < t \leqq \frac{\pi}{\omega_0})$$

(see Fig. 5)

2-5 Axial Drift

With $\dot{z}_0 = 0$, from (4) (taking $z_0 = 0$)

$$Z = -\frac{e}{m}\int_0^t \{A_z(r(t)) - A_z(r_0)\}dt \tag{26}$$

With the same approximation used in 2-4, the first order solution of z is obtained by using the zero order r, (24) and (25) in the right side of (26). The particle deviates from the zero-order orbit (later we call the standard orbit) after one Larmor rotation by

$$Z = -\frac{e}{m}\left[\int_0^{\frac{\pi}{2\omega_0}} \{A_z(r) - A_z(r_0)\}dt - \int_{\frac{\pi}{2\omega_0}}^{\frac{\pi}{\omega_0}} \{A_z(r) - A_z(r_0)\}dt\right.$$

$$= -\frac{2e}{m}\int_{r_0}^{0} \{A_z(r) - A_z(r_0)\}\frac{dr}{\dot{r}_{(0)}} \tag{27}$$

which remains a positive definite value in a usually expected current distribution and does not cancel out as has been considered. The circumstance will be clear in Fig. 6.

(Note: Even in the case $\dot{z}_0 \neq 0$, the axial deviation of the particle from the standard orbit is still given by (26))

2-6 Numerical Examples

1. Radial drift

We shall give some numerical examples of the deviation from the standard orbit after one Larmor rotation with $\dot{r}_0 = 0$ and $r_0 = a$,

(a) case 1. With the distribution of (10),

$$A_z(r)-A_z(r_0)=\frac{\mu_0 j_0}{2(n+2)a^n}(a^{n+2}-r^{n+2})$$

and

$$B_p=\frac{\mu_0}{2}j_0 a\cos^{n+1}\omega_0 t$$

$$\therefore\quad \dot{r}_{(1)}=-\frac{e}{m}\dot{Z}_0\mu_0\frac{j_0}{2}a\int_0^t\cos^{n+1}\omega_0 t\,dt$$

$$=-\frac{e}{m}\dot{Z}_0\mu_0\frac{a j_0}{2\omega_0}\begin{cases}\dfrac{1}{2^{2p}}\left[\sum_{i=0}^{p-1}\binom{2p}{i}\dfrac{\sin 2(p-i)\omega_0 t}{p-i}\right. \\ \qquad\left.+\binom{2p}{p}\omega_0 t\right. & \text{for}\quad n+1=2p \\ \dfrac{1}{2^{2p}}\sum_{i=0}^{p}\binom{2p+1}{i}\dfrac{\sin(2p-2i+1)\omega_0 t}{2p-2i+1} & \text{for } n+1=2p+1\end{cases} \tag{28}$$

For $n=0$,

$$\dot{r}_{(1)}=-\mu_0\frac{e}{m}\dot{Z}_0\frac{j_0}{2}a\frac{\sin\omega_0 t}{\omega_0}$$

$$\therefore\quad \dot{r}_{(1)}\Big|_{r=0}=\dot{r}_{(1)}\Big|_{t=\frac{\pi}{2\omega_0}}=-\mu_0\frac{e}{m}\dot{Z}_0\frac{j_0}{2}\frac{a}{\omega_0}$$

The radial deviation Δr is

$$|\Delta r|=\frac{\pi}{\omega_0}|\dot{r}_{(1)}|_{r=0}=\frac{\mu_0\pi e}{2m}\cdot\frac{\dot{Z}_0 j_0}{\omega_0^2}a=|\Delta r|_{n=0} \tag{29}$$

In a similar way,

$$\frac{|\Delta r|}{|\Delta r|_{n=0}}=0.785 \quad \text{for } n=1$$

$$=0.667 \quad =2$$

$$=0.589 \quad =3$$

$$=0.533 \quad =4$$

b) case 2. With the distribution of (13)

$$B_p = \mu_0 \frac{p+2}{p} j_0 a \left(\frac{\cos\omega_0 t}{2} - \frac{\cos^{p+1}\omega_0 t}{p+2} \right)$$

$$\therefore \quad \dot{r}_{(1)} = -\frac{p+2}{p} \frac{e}{m} \dot{Z}_0 \mu_0 \frac{j_0}{2} a \left(\frac{1}{2}\int_0^t \cos\omega_0 t\,dt - \frac{1}{p+2}\int_0^t \cos^{p+1}\omega_0 t\,dt \right)$$

$$= -\mu_0 \frac{p+2}{2p} \frac{e}{m} \dot{Z}_0 j_0 \frac{a}{\omega_0} \left(\sin\omega_0 - \frac{1}{p+2} \right.$$

$$\times \begin{cases} \dfrac{1}{2^{2p'}} \left(\displaystyle\sum_{i=0}^{p'-1} \binom{2p'}{i} \frac{\sin 2(p'-i)\omega_0 t}{p'-i} + \binom{2p'}{p'} \omega_0 t \right) \\ \qquad\qquad \text{for} \qquad p+1 = 2p' \\ \dfrac{1}{2^{2p'}} \displaystyle\sum_{i=0}^{p'} \binom{2p'+1}{i} \frac{\sin(2p'-2i+1)\omega_0 t}{2p'-2i+1} \\ \qquad\qquad \text{for} \qquad p+1 = 2p'+1 \end{cases} \qquad (29)$$

For $p = 1$,

$$\dot{r}_{(1)}\Big|_{t=\frac{\pi}{2\omega_0}} = -3\mu_0 \frac{e}{2m} \dot{Z}_0 j_0 \frac{a}{\omega_0} \left(\sin\omega_0 t \Big|_{t=\frac{\pi}{2\omega_0}} - \frac{1}{3} \times \right.$$

$$\left. \left| \frac{1}{4}\sin 2\omega_0 t + \frac{\omega_0}{2} t \right|_0^{\pi/2\omega_0} \right)$$

$$= -\frac{3}{2}\mu_0 j_0 \dot{Z}_0 \frac{e}{m} \frac{a}{\omega_0} \left(1 - \frac{1}{3} \times \frac{\pi}{4} \right)$$

$$= -\mu_0 \frac{e}{2m} \dot{Z}_0 j_0 \frac{a}{\omega_0} \times 2.21$$

The radial deviation is

$$|\Delta r| = 2.21 \, |\Delta r|_{n=0}$$

$$\frac{|\Delta r|}{|\Delta r|_{n=0}} = 1.67 \qquad \text{for } p = 2$$

$$= 1.14 \qquad p = 3$$

The absolute value of the deviation is evaluated with the parameters in a Tokamak device in JAERI (JFT-2)[3],

$$B_z = 1.5 \text{ Wb/m}$$
$$I = 250 \text{ kA}$$
$$a = 0.25 \text{ m}$$

, supposing α - particles from Po^{210}, as follows:

$$|\Delta r|_{n=0} = 30.5 \text{ cm}.$$

2. Axial drift

case 1.

$$\Delta Z = \frac{e}{m} \frac{\mu_0 j_0}{\omega_0 2(n+2)a^n} \oint \frac{a^{n+2} - r^{n+2}}{\sqrt{a^2 - r^2}} dr$$

$$= \frac{e}{m} \frac{\mu_0 j_0 a^2}{\omega_0 (n+2)} \int_1^0 \frac{1-u^{n+2}}{\sqrt{1-u^2}} du \qquad (30)$$

Using the formula

$$\int_1^0 \frac{1-u^{n+2}}{\sqrt{1-u^2}} du = -\frac{\pi}{2} + \begin{cases} \dfrac{\pi(2p)!}{2^{2p+1}} \dfrac{1}{(p!)^2} & \text{for} \quad n+2 = 2p \\ \dfrac{2^{2p}(p!)^2}{(2p+1)!} & \text{for} \quad n+2 = 2p+1 \end{cases}$$

We get

$$\frac{\Delta Z}{\left[\frac{e}{m} \frac{\mu_0 j_0}{\omega_0} a^2\right]} = -0.393 \quad \text{for } n = 0$$
$$= -0.300 \quad n = 1$$
$$= -0.246 \quad n = 2$$
$$= -0.207 \quad n = 3 .$$

With the parameters of JFT-2,

$$\frac{e}{m} \frac{\mu_0 j_0 a^2}{\omega_0} = 0.133 \text{ m}$$

2-7 Choice of one of the two methods

Now we have two possibilities in the measurement of plasma current distribution, that is, by a radial and an axial drift.

The choice of one of two should depend on the convenience of the actual arrangements of the experiment. At present it seems to us that

the observation of the axial drift is better in our experiment, noting several following facts:

1) The estimated radial drift is too large to be measured in the observation port (6 cm in width. See Fig. 7).

2) The ports in which α - particle source and detectors should be set are located with an angle of $\pi/2$ with each other, and it limits the energy of the particle in several discrete values (See Fig. 8).

3) For $\dot{z}_0 \neq 0$ the drifts in two directions are expected and the detectors should be arranged in a two- dimensional space, for example, in a form of a mesh. It will make the system too complicated and cost so much.

Later we shall choose the axial drift which is estimated to be 5.23 cm for n = 0 and sufficiently large for our purpose.

2-8 Measurement by the other standard orbit

In the real experimental arrangement, the α - source and the detector should not necessarily be set on the surface of the plasma column, but a little apart from that. In that case we have to use the orbit of a larger radius than (24) and (25). (See Fig. 9). All above discussions stand with minor modification for the new standard orbit.

The axial drift (30) is changed only as

$$\Delta Z=\frac{e}{m\omega_0}\int_a^0 \frac{\mu_0 j_0}{(n+2)a^n}\cdot\frac{a^{n+2}-r^{n+2}}{\sqrt{r_1^2-r^2}}\,dr \tag{31}$$

, which is the deviation suffered in the period when the particle is injected into the plasma and returns to the surface, and r_1 is the radius of the new standard orbit.

From (31),

$$\Delta Z=\frac{e}{m}\,\frac{\mu_0 j_0}{\omega_0(n+2)a^n}\,r_1^{n+2}\int_{\frac{a}{r_1}}^0\left(\frac{a^{n+2}}{r_1^{n+2}}-u^{n+2}\right)\Big/\sqrt{1-u^2}\,du \tag{32}$$

Noting that

$$\int_{a/r_1}^0\frac{\frac{a^{n+2}}{r_1^{n+2}}-u^{n+2}}{\sqrt{1-u^2}}\,du=\frac{a^{n+2}}{r_1^{n+2}}\int_{\frac{a}{r_1}}^0\frac{du}{\sqrt{1-u^2}}-\int_{\frac{a}{r_1}}^0\frac{u^{n+2}}{\sqrt{1-u^2}}\,du \tag{33}$$

and the second integral on the right side of (33) is

$$-\sum_{r=0}^{m}\left\{\frac{(2m-1)(2m-3)\cdots(2m-2r+1)}{2m(2m-2)\cdots\cdots(2m-2r)}u^{2m-2r-1}\right\}\sqrt{1-u^2}\Bigg|_{\frac{a}{r_1}}^{0}$$
$$+\frac{(2m-1)(2m-3)\cdots 1}{(2m)\cdots\cdots 2}\sin^{-1}u\Bigg|_{\frac{a}{r_1}}^{0}$$

for $n+2=2m$

$$-\sum_{r=0}^{m}\left\{\frac{2m(2m-2)\cdots(2m-2r+2)}{(2m+1)\cdots(2m-2r+1)}u^{2m-2r}\right\}\sqrt{1-u^2}\Bigg|_{\frac{a}{r_1}}^{0}$$

for $n+2=2m+1$

for $n = 0$ the drift Δz is

$$\Delta Z=\frac{e}{m}\frac{\mu_0 j_0}{2\omega_0}r_1^2\left\{\frac{a^2}{r_1^2}\left(-\sin^{-1}\frac{a}{r}\right)-\frac{1}{2}\frac{a}{r_1}\sqrt{1-\frac{a^2}{r^2}}+\frac{1}{2}\sin^{-1}\frac{a}{r_1}\right\} \tag{34}$$

For α - particle from Po^{210},

$$\Delta z = -5.79 \text{ cm}$$

and it is of the same order as in the case of the standard orbit.

2-9 Measurement with multiple α - beams

Returning to the standard orbit, the axial drift Δz is a function of the injected angle or the initial radial velocity $\dot{r}_0$. We may measure the plasma current distribution without assuming its radial dependence at the same time using multiple α - beams with various values of $\dot{r}_0$.

Instead of $\dot{r}_0$, r_{min} is taken as a parameter as shown in Fig. 9.

In order to get the drift Δz for the orbit with a definite r_{min}, the orbit is represented with the polar co-ordinates in Fig. 10, as

$$r^2=\left(\frac{a+2r_{min}}{a}\right)a^2\cos^2\omega_0 t+r_{min}^2$$

$$\therefore\ \frac{dr}{dt}=-\frac{\omega_0(r^2-r_{min}^2)^{1/2}\{(a+r_{min})^2-r^2\}^{1/2}}{r} \tag{35}$$

The drift Δz is

$$\Delta Z(r_{min}) = \frac{2e}{m}\int_a^{r_{min}} \{A_z(r) - A_z(a)\}\frac{dr}{\dot{r}}$$

$$= \frac{2e}{m}\int_a^{r_{min}} \frac{r}{\sqrt{r^2 - r_{min}^2}\sqrt{(a+r_{min})^2 - r^2}} \{A_z(r) - A_z(a)\} dr \quad (36)$$

(36) is a first kind Volterra type integral equation, related to an unknown function $A_z(r) - A_z(a)$ and the kernel function $K(r, r_{min})$ is

$$K(r, r_{min}) = \frac{r}{(r-r_{min})^{1/2}\left[(r+r_{min})\{(a+r_{min})^2 - r^2\}\right]^{1/2}} \quad (37)$$

$r = d$ is the only singular point in the region $d \leqq r \leqq a$ of the order $1/2$, and (36) is the generalized Abel integral equation with $\alpha = 1/2$. The equation has a unique solution which determines the current distribution.

(36) cannot be solved analytically, it, however, is transformed into the following Volterra type integral equation,

$$\pi \frac{r_{min}\{A_z(r_{min}) - A_z(a)\}}{(2r_{min})^{1/2}\{(a+r_{min})^2 - r_{min}^2\}^{1/2}} + \int_a^{r_{min}} \frac{\partial X(r_{min}, r)}{\partial r_{min}}$$

$$\{A_z(r) - A_z(a)\} dr = \frac{\partial}{\partial r_{min}} \int_a^{r_{min}} Z(s) \frac{ds}{(s - r_{min})^{1/2}} \quad (38)$$

and it may be solved by a successive approximation, where

$$\frac{\partial X(r_{min}, r)}{\partial r_{min}} = \int_0^1 \frac{1}{t^{1/2}(1-t)^{1/2}} \frac{\partial}{\partial d}\left[\frac{r}{\{2r + (d-r)t\}^{1/2}}\right.$$

$$\left. \times \frac{1}{\{(a+r+(d-r)t)^2 - r^2\}^{1/2}}\right] dt$$

2-10 Resolution

There are several causes which result in the definite width in the axial drift spectrum as a function of r_{min}, as

1) A definite dimension of α - source.
2) Velocity spread of α - ray around $\dot{z}_0 = 0$.

3) Energy spread.

(1) Effect of the size of α - source on the deviation spectrum

α - source can have three dimensional spread, δr, $\delta\theta$ and δz.

Among them, only δr is worthly for noting because $\delta\theta$ and δz produce the spectrum width of the same value, that is, $\delta\theta$ and δz respectively according to the symmetry of the problem.

For simplicity we assume that $A_z(r) - A_z(a)$ in (36) is expanded by a series of polynomials of even order, and here the simplest case $j = j_0$ is studied.

The vector potential is

$$A_z(r) - A_z(a) = \frac{\mu_0 j_0}{4a^2}(a^2 - r^2)$$

and the drift is

$$\Delta Z = \frac{e\mu_0 j_0}{4m\omega_0} \int_{a^2}^{r_{min}^2} \frac{a^2 - u}{\sqrt{(u - r_{min}^2)\{(a + r_{min}^2) - u\}}} \tag{39}$$

Because

$$\int_{a^2}^{r_{min}^2} \frac{udu}{\sqrt{(u - r_{min}^2)\{(a + r_{min})^2 - u\}}} = -2a^2 \tan^{-1} \sqrt{\frac{a^2 - r_{min}^2}{(a + r_{min}^2) - a^2}}$$

and

$$\int_{a^2}^{r_{min}^2} \frac{udu}{\sqrt{(u - r_{min}^2)\{(a + r_{min})^2 - u\}}} = \sqrt{(a^2 - r_{min}^2)\{(a + r_{min})^2 - a^2\}} - \{(a + r_{min})^2 + r_{min}^2\} \tan^{-1} \sqrt{\frac{a^2 - r_{min}^2}{(a + r_{min})^2 - a^2}}$$

the drift is

$$\Delta Z = \frac{e\mu_0 j_0}{4m\omega_0} a^2 \left[-2 \tan^{-1} \sqrt{\frac{1 - k^2}{k(2 + k)}} - \sqrt{(1 - k^2)k(2 + k)} + (1 + 2k + 2k^2) \tan^{-1} \sqrt{\frac{1 - k^2}{k(2 + k)}} \right. \tag{40}$$

where $k=\frac{r_{min}}{a}$

The derivative of z to k is

$$\frac{dz}{dk}=\frac{e}{4m\omega_0}\mu_0 j_0 a^2\left[\frac{-2k^{1/2}(2+k)^{1/2}(1-k^2)^{1/2}}{2k+1}+2(1+2k)\tan^{-1}\sqrt{\frac{1-k^2}{k(2+k)}}\right]$$

The fractional width of the spectrum dz/z caused by the deviation of the source position, δr in the radial direction is

$$\frac{dz}{z}=\frac{dz}{dk}\frac{\delta r}{az}\left[\frac{-2\{k(2+k)(1-k^2)\}^{1/2}}{2k+1}+2(1+2k)\tan^{-1}\sqrt{\frac{1-k^2}{k(2+k)}}\right]$$
$$\times\left[-2\tan^{-1}\sqrt{\frac{1-k^2}{k(2+k)}}-\sqrt{(1-k^2)k(2+k)}\right.$$
$$\left.+(1+2k+2k^2)\tan^{-1}\sqrt{\frac{1-k^2}{k(2+k)}}\right]^{-1}\frac{\delta r}{a} \qquad (41)$$

(41) is evaluated for k = 1/2, for example, as

$$\left.\frac{dz}{z}\right|_{k=1/2}=1.49\frac{\delta r}{a}$$

(2) Effect of definite initial axial velocity

It is convenient to use the co-ordinate shown in Fig. 11. Lagrangian L in this co-ordinate is

$$L=\frac{m}{2}\{\dot{r}^2+\dot{z}^2+(r\dot{\varphi})^2\}+e(\dot{r}A_\varphi+\dot{z}A_z+r\dot{\varphi}A_\varphi)$$

and the momentum in the φ - direction must be conserved:

$$2r^2\dot{\varphi}=\text{const}=2r_0^2\dot{\varphi}_0$$

$$\therefore\ \dot{\varphi}=\left(\frac{R+a}{r}\right)^2\dot{\varphi}_0$$

Usually the approximation $a \ll R$ is proper in a Tokamak device so that no focusing character can be expected in φ - direction.

With zero order approximation, $\dot{\varphi}$ should be taken constant and the spread of the z spectrum is

$$\int_0^t r\dot{\varphi}dt \simeq \int_0^t \dot{z}_0 dt$$

For the standard orbit

$$\frac{\delta z}{z} \simeq \frac{\dot{z}_0 \frac{\pi}{\omega_0}}{z}$$

(3) Effect of the energy spread

The effect of the energy spread on the z - spectrum is divided into two parts: by the shift of the injection angle and by the change of r_{min}. The former is already evaluated in 2-8 and fairly small. The latter is easily evaluated with δE as

$$\frac{\delta E}{z} = 4 \frac{\delta r_{min}}{a}$$

so

$$\frac{\delta z}{z} = \frac{1}{4} \frac{\delta E}{E}$$

2-11 Toroidal effect

The real machine has a toroidal curvature (see Fig. 11) which causes the drift of the particles perpendicular to the external magnetic field and the toroidal axis. Its velocity v is

$$v = \left| \text{grad ln } B \right| \frac{E}{eB} \qquad (42)$$

and for the standard orbit the drift in the vertical direction is

$$v \cdot \frac{\pi}{\omega_0} \sim 5 \text{ cm} \qquad \text{(see Fig. 12)}$$

This is about one fifth of the plasma radius and may not change the disscussions in the linear geometry. In the toroidal geometry the particle motion in a limit of zero plasma current - zero order solution - is obtained by the equations

$$m\ddot{r} = -e\dot{z}B_0 \frac{r}{R}$$

$$m\ddot{z} = e\dot{r}B_0 \frac{r}{R}$$

where the co-ordinates are shown in Fig. 12, which give the solution

$$\int_a^r \frac{dr}{\left[-\frac{2eB_0}{m^2R}\left\{-\frac{eB_0}{8R}r^4+\frac{c_1}{2}r^2\right\}+\frac{2c_2}{m}\right]^{1/2}}=t \tag{44}$$

This is an elliptic function and it is quite possible to repeat the analysis in the case of linear geometry with use of the solution of (44) to obtain the first order solution in the toroidal case, although the process will be rather complicated and the numerical calculation will be better caried out.

3. α - Beam Spread with Collisions with the Plasmas

There are several more factors which contribute to the width in the axial drift spectrum through the energy spread. One of them is the collision of the α - particles with other material standing on the way from the source to the detector - the plasma particles itself or the coating of the source which is necessary for shielding it against the back-ground radiations.

The spread of the beam velocity in the perpendicular direction to the beam is by Spitzer[4)]

$$<(\Delta v_\perp)^2>=\frac{d}{dt}<(v_\perp^2)>=\frac{A_D}{v}\{\Phi(\ell_f v)-G(\ell_f v)\} \tag{45}$$

where A_D is a diffusion constant and

$$A_D=\frac{e^4 m_f z^2 z_f^2 \ell n\Lambda}{2\pi\varepsilon_0^2 m^2} \tag{46}$$

and $\Phi(\ell_f v)$ is an error function,

$$\Phi(x)=\frac{2}{\pi^{1/2}}\int_0^x e^{-y^2}dy \tag{47}$$

$G(x)$ is

$$G(x)=\frac{\Phi(x)-x\Phi'(x)}{2x^2} \tag{48}$$

where m : the mass of the injected ion

Ze : the charge of the injected ion

$Z_f e$: the charge of the plasma ion

v : the velocity of the injected ion

$v_\perp$: the perpendicular velocity of the injected ion

l_f^2 : $\dfrac{m_f}{2kT_f}$

The perpendicular spread of the injected ion beam, $\langle r^2 \rangle$, where r is the co-ordinate perpendicular

$$r = \int_0^t v_\perp(t')\,dt'$$

is given by

$$\langle r^2 \rangle = \left\langle \int_0^t v_\perp(t')\,dt' \int_0^t v_\perp(t'')\,dt'' \right\rangle \tag{49}$$

$$= \int_0^t dt' \int_0^t dt'' \langle v_\perp(t') v_\perp(t'') \rangle$$

$$\simeq \frac{t^2}{2} \langle v_\perp^2(\frac{t}{2}) \rangle \tag{50}$$

where we evaluate the value of $v_\perp(t')$, $v_\perp(t'')$ at $t', t'' = t/2$, considering that $v_\perp^2(t)$ is a monotoneously increasing function of t. (50) is rewritten with $\langle (\Delta v_\perp)^2 \rangle$ as

$$\langle r^2 \rangle \simeq \frac{t^3}{4} \langle (\Delta v_\perp)^2 \rangle \tag{51}$$

noting that $\langle (\Delta v_\perp^2) \rangle$ is the rate of increase of $\langle v_\perp^2 \rangle$.

From (45) and (51),

$$\langle r^2 \rangle \simeq t^3 \frac{e^4 n_f z^2 z_f^2 \ell n \Lambda}{8\pi m^2 v} (\Phi - G) \tag{52}$$

Substituting $t = 1/v$ where l is the total length of the orbit into (52), and taking into account two species of particles in plasmas

$$\langle r^2 \rangle = \ell^3 \frac{e^4 n_f z^2 z_f^2 \ell n \Lambda}{8\pi m^3 v^4} \sum_{i,e} (\Phi - G)$$

$$= \frac{\ell^3}{2^{1/2}\pi^2} \left(\frac{\pi e^4}{m^{1/2} E^{3/2}}\right) \left(\frac{n_f z^2 z_f^2 \ell n \Lambda}{v}\right) \sum_{i,e} (\Phi - G)$$

where E is the kinetic energy of the injected particle (α) and inserting numerical values,

$$\langle r^2 \rangle (m^2) = \frac{\ell^3 (m) n_f (m^{-3}) z^2 z_f^2 \ell n \Lambda \Sigma (\Phi - G) \times 0.164 \times 10^{-17}}{E^2 (ev)} \qquad (53)$$

The value of ln Λ is about 15 in our Tokamak device[2], and $\Phi - G$ is near unity because

$$\frac{v}{\sqrt{\frac{2kT_i}{m_H}}} >> 1$$

for the collision between α - particle and the ions of plasma (H^+) with the ion temperature T_i, and about 0.5 for the collision between α and the electrons with

$$\frac{v}{\sqrt{\frac{2kT_e}{m_e}}} \simeq 0.83$$

supposing α - rays emitted from the usually available isotopes (E 5 MeV) and the plasma of the ion and electron temperatures of 500 and 1000 eV respectively.

Then (53) becomes

$$\langle r^2 \rangle = 3.7 \times 10^{-17} \frac{\ell^3 n_f z^2 z_f^2}{E^2}$$

With the numerical values,

$l = 1$ m

$n_f = 5 \times 10^{19}$ m^{-3}

$E = 5$ MeV

$Z = 2$

$Z_f = 1$

$$\langle r^2 \rangle \simeq \frac{3.7 \times 4}{5 \times 10^6} \times 10^{-4} = 3 \times 10^{-10} m^2$$

$$\therefore \sqrt{\langle r^2 \rangle} = 1.7 \times 10^{-3} \text{ cm}$$

As stated in the previous sections, the axial drift of α - particles is estimated to be the order of a few cm and the collision with the plasma particles will give the spectrum width of about 0.1% which may be negligible.

4. Energy Loss and Energy Spread of α - particles due to Instrumental Causes

Besides the collision with the plasma, α - particles will lose their energy due to some phenomena such as the self - absorption by the α - source itself having a finite thickness, the passage through a thin layer of the light shield set on the surface of the source and the detector.

Extensive measurements have been made of the range - energy relationship of α - particles in air. One of emprical equations got from the measurements, which fits with better than 1% accuracy in the range from 4 to 11 MeV is

$$R = (0.005E + 0.285)\, E^{3/2} \tag{54}$$

where R is the mean range in centimeters at normal conditions and E is the α - particle energy in MeV. For different absorbing materials, it is known that the quantity $R\rho/\sqrt{A}$ is approximately constant for a given energy particle, and ρ and A are the material's density and atomic weight, respectively. Thus

$$\frac{R_1}{R_0} \sim \frac{\rho_0}{\rho_1}\,\frac{\sqrt{A_1}}{\sqrt{A_0}} \tag{55}$$

where the subscripts 0 and 1 refer each to a different absorbing material. By substituting in the values for air of

$$\rho_0 = 1.226 \times 10^{-3}\ g/cm^3$$

and $\sqrt{A_0} = 3.82$ (55) becomes

$$R_1\,(cm) \simeq 3.2 \times 10^{-4}\,\frac{\sqrt{A_1}}{\rho_1\,(g/cm^3)}\,R_{air}\,(cm)$$

For example, for the α - particle of 5.3 MeV from Po^{210}, the range is 38 mm in the air and therefore 11.6, 8.8 and 23.4 μm in the stainless steel, gold and alminium foil respectively.

These values are far beyond the technical limit which is expected to be realizable for the usual shield foil and we may have no serious problem.

The energy loss of a charged particle in matter is essentially a statistical phenomenon. Particles of a given kind and of a given

energy do not all lose exactly the same amount of energy in traversing a given thickness of material, but we can discuss only the probability that a particle of initial energy E_0 has an energy between E and E + dE after traversing a thickness of x $g \cdot cm^{-2}$ of matter, $\omega(E_0, E, x)$. Symon gave the probability in a complete form. In his treatment $\omega(E_0, E, x)$ has a maximum at $E = E_p(x)$, so called the most probable energy loss, and the half value width of the distribution curve is about 2.5 Δ_0 with a little dependence on λ, where

$$\Delta_0 = \frac{2Cm_e c^2 x}{\beta^2} b$$

and

$$C = 0.150 \frac{Z}{A} g^{-1}\ cm^2$$

b and λ are the functions of $\beta = \frac{v}{c}$ and G, where

$$G = \frac{2Cm_e c^2 x}{\beta^2 E'_m}$$

and

$$E'_m = 2m_e c^2 \frac{\beta^2}{1-\beta^2}$$

The relations of b and λ to G with a parameter β are given graphically in Symons' paper.

Inserting the numerical values into these equations, we get

$$G \simeq 8$$

for stainless steel foil of 1 μm thick, and then $b \sim 0.35$.

Therefore

$$\Delta_0 \simeq 0.024 \text{ MeV}$$

and we expect the energy spread of the order of 0.05 MeV in the energy of α - particles traversing 1 μm thick stainless steel foil. It corresponds to about 1% of the total energy and so the foil thickness will be allowable.

5. Selection of α - Source

In a practical point of view, the utilizable α - sources are rather limited. The candidates are shown in the Table 1 with their main characteristics.

(1) Po^{210} Po^{210} has several marits as α - emitter. The half-life is sufficiently long and it has a high specific activity which may result in the source in a form of a very thin layer, and the self-absorption by the source itself will be small. Moreover it has no γ - emission which might produce a serious shielding problem. On the contrary, its chemical characteristics are not so much favourable. It is volatile and diffusive so that it requires severe techniques in treating it.

(2) Pb^{212} It is produced by the following process:

$$Th^{228} \rightarrow Rn^{220} \rightarrow Pb^{212}$$

In the last step, it must be separated radiochemically, and the technique for separation should be settled. Th^{228} is not easy to be got commercially due to its property as the nuclear fuel. Pb^{212} emits γ - ray with α, so that the system for shielding may be bulky. It is, however, neither volatile, nor diffusive.

(3) Am^{241} This radioisotope has a relatively low specific activity and the energy spread by the self-absorption may be great. It is accompanied with low energy γ - radiation.

(4) Cm^{242} α - particles of the different energies are emitted. At present very few laboratories produce the radioisotope and its importation must be arranged. It may be treated easily with the ordinary chemical technique.

It can not be decided which is the most favourable source only by comparing the characters of these sources, but it must be discussed related to the other problems of the experimental set up, for example, the required accuracy of measurement, the counting rate of the α - particles and the choice of the detector. At present, so far as we assume small background noise, Cm^{242} seems to be promising, due to its easy care of the treatment.

6. Detector System and Counting Rate

A solid state detector called "Nuclear Triode" by Nuclear Diodes Inc. is a leading candidate. Two pulses respresenting the energy and the position of the injected particle respectively are obtained simultaneously from the detector. The effective area of the detector is sufficiently large and reaches 4 x 20 mm at maximum. We might use the well-known coincidence technique to reduce the spurious signal, although it is not so clear whether the detector is the most desirable.

We expect the counting rate of the order of 1 pulse per every msec. The number of α - particles n impinging with the detector the solid angle of which is $\Delta\Omega$ for the α - source is in a time interval Δt

$$n = 3.7 \times 10^{10} S \, \Delta t \, \Delta\Omega \, sec^{-1}$$

where s is the source intensity in Curie. With the numerical values given previously and supposing the detector of the sensitive area of 0.8 cm^2 (4 x 20 mm), $\Delta\Omega$ is about 0.5 x 10^{-4} steradian and the source intensity which is necessary for the counting rate of 10^3 (1 pulse/msec) is

$$s \simeq 0.55 \text{ mC}$$

We will have one signal pulse per one α - particle and it is not desirable to use a large quantity of the source to avoid the pile up of the signal. The schematic experimental arrangement is shown in Fig. 13.

Reference

1) K. Inoue and T. Takeda: JAERI-memo 4236, unpublished Dec. (1970)

2) T. Tamano: Private communication

3) S. Itoh et al: JAERI-memo 4084, July (1970)

4) Lyman Spitzer, Jr.: "Physics of Fully Ionized Gases". Interscience Publishers Inc. New York, (1956)

α -emitter	Energy of (fractional rate) MeV. (%)	Half Life days	γ -emission	Chemical Characters	Note
P_o^{210}	5.3 (99) 4.5 (10^{-3})	138.4	no	Volatile diffusive	$B_i^{209} \rightarrow B_i^{210} \rightarrow P_o^{210}$
P_b^{212}				-	$T_h^{228} \rightarrow R_n^{220} \rightarrow P_b^{212}$ not easy to import
A_m^{241}	5.48 (84) 5.43 (14) 5.38 (1.4) 5.54 (0.3) 5.50 (0.2)	458 (y)	Low energy γ	-	
C_m^{242}	6.11 (73.7) 6.01 (26.3) 5.96 (0.04)	162.5			easy to treat

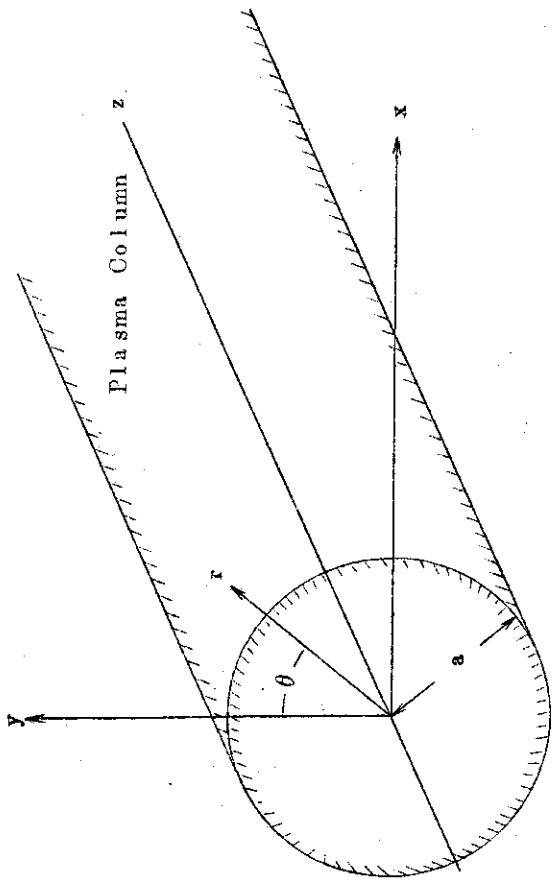

Fig. 1 Plasma Column in Linear Geometry.
External field is applied in z-direction externally.
Plasma current is supposed to flow in z-direction
and with axial symmetry.

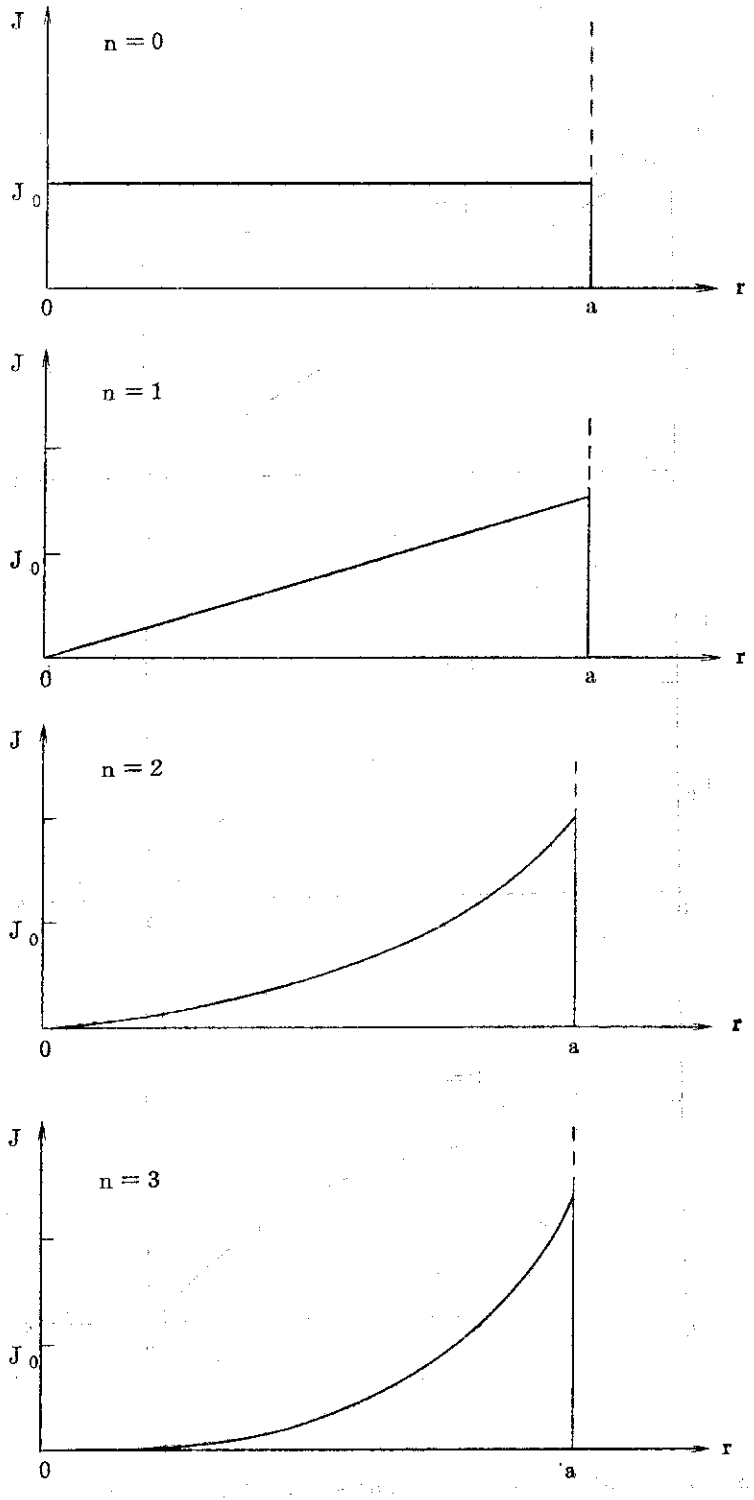

Fig. 2 Assumed Distributions of Plasma Current with Positive r-Dependence.

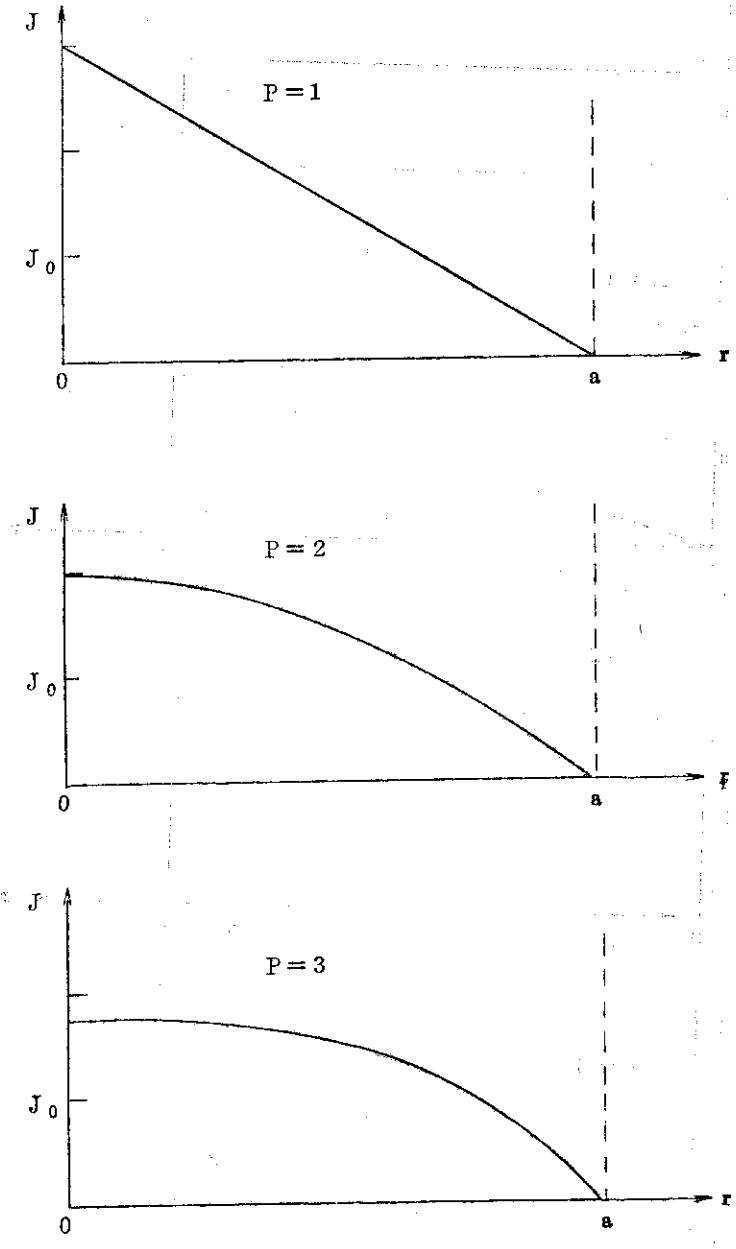

Fig. 3 Assumed Distributions of Plasma Current with Negative r-Dependence.

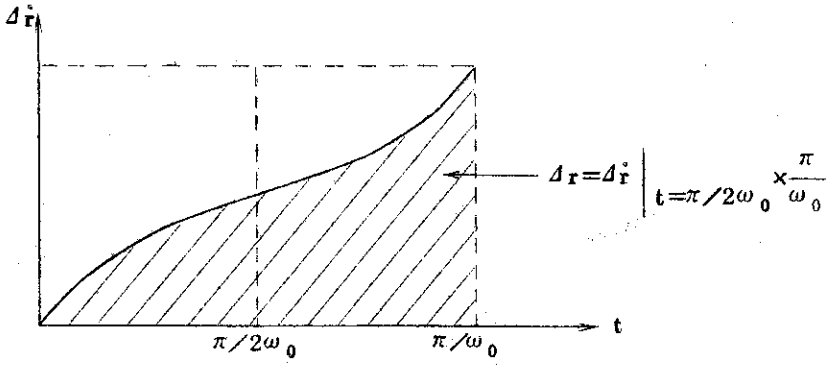

Fig. 4 Deviation of α-velocity in r-direction from the standard case by plasma current. The area of the shaded region represents the radial deviation.

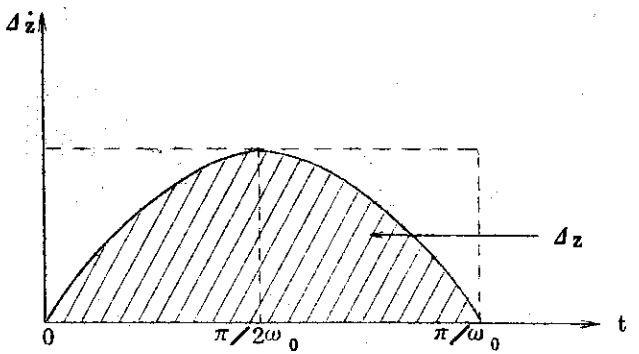

Fig. 6 Deviation of α-velocity in z-direction from the standard case by plasma current. The velocity deviation vanished after one period of the Larmor rotation, but r-deviation still remains.

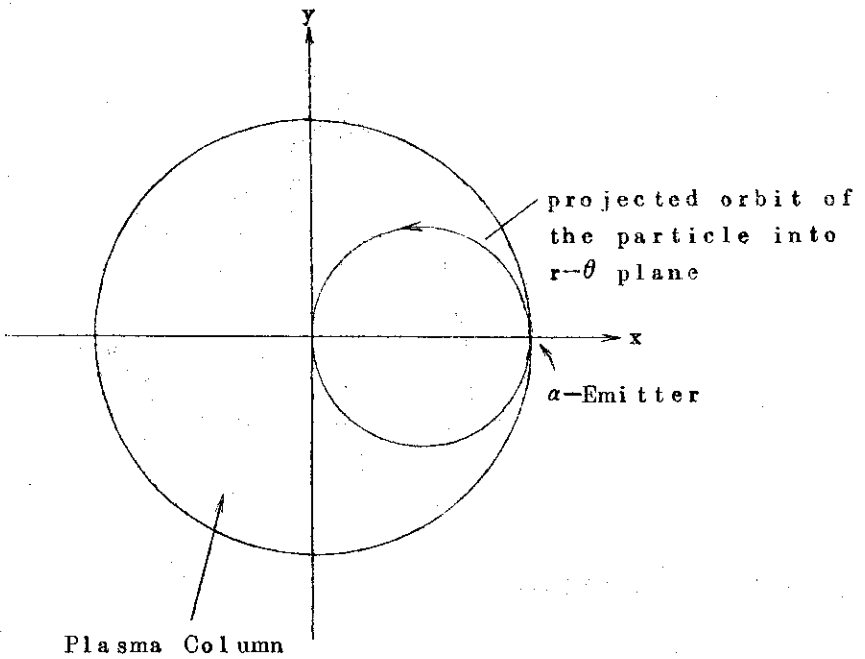

Fig. 5 Standard Orbit.
The external magnetic field is perpendicular to the paper from the surface to the back.

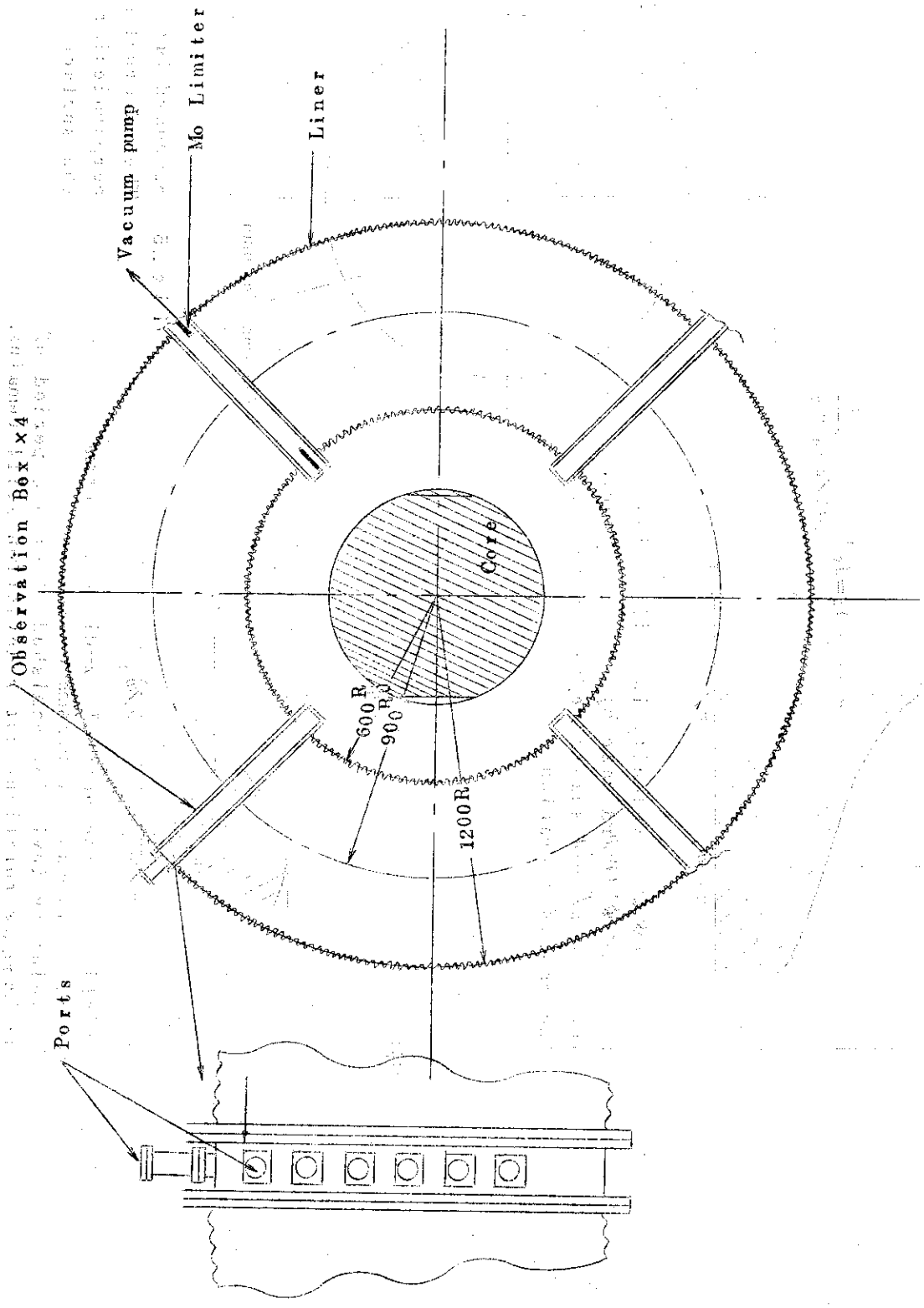

Fig. 7 Arrangement of Observation Ports in JFT-2.

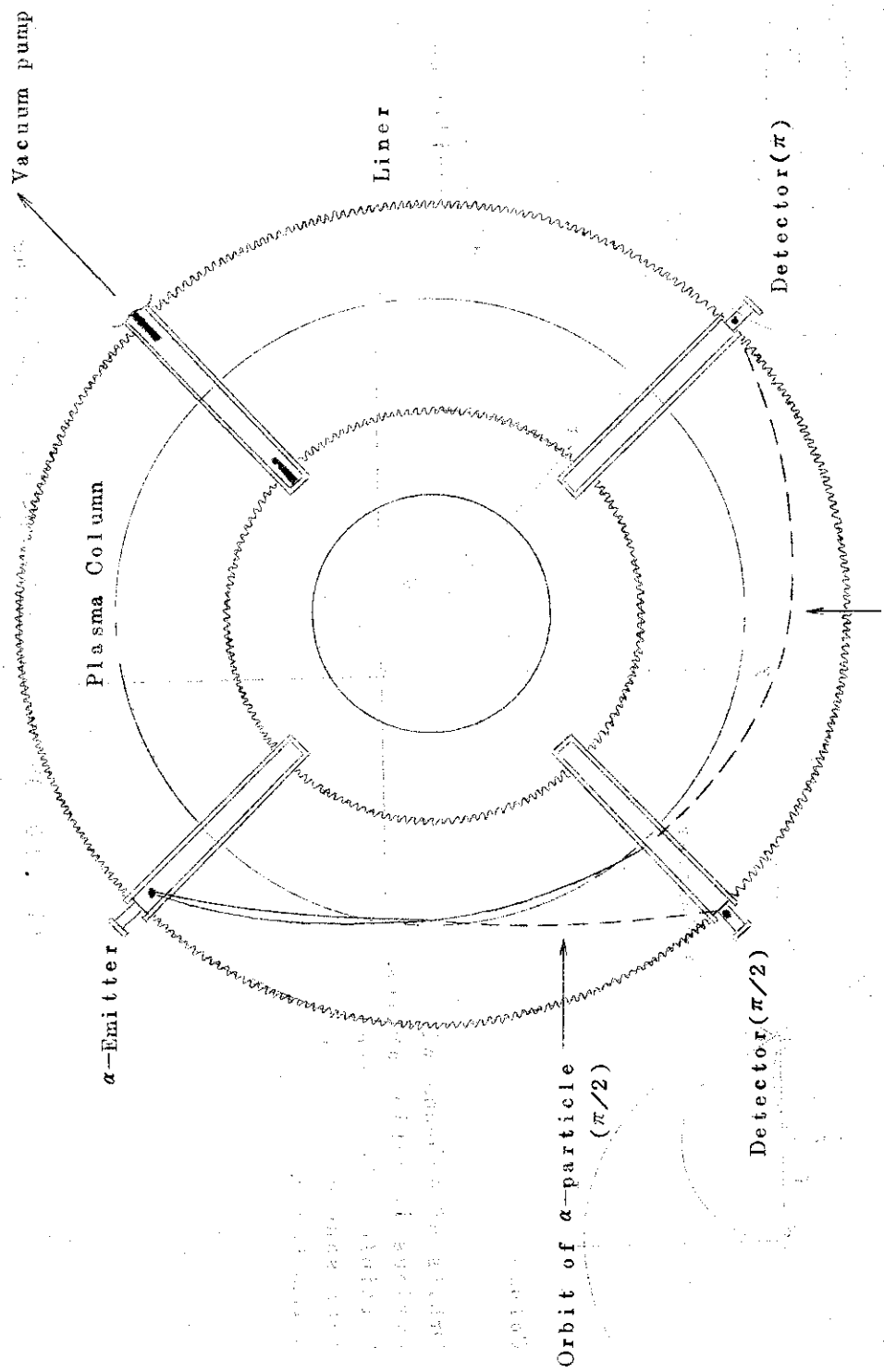

Fig.8 Orbits of α-particles Projected to r-φPlane in JFT-2.

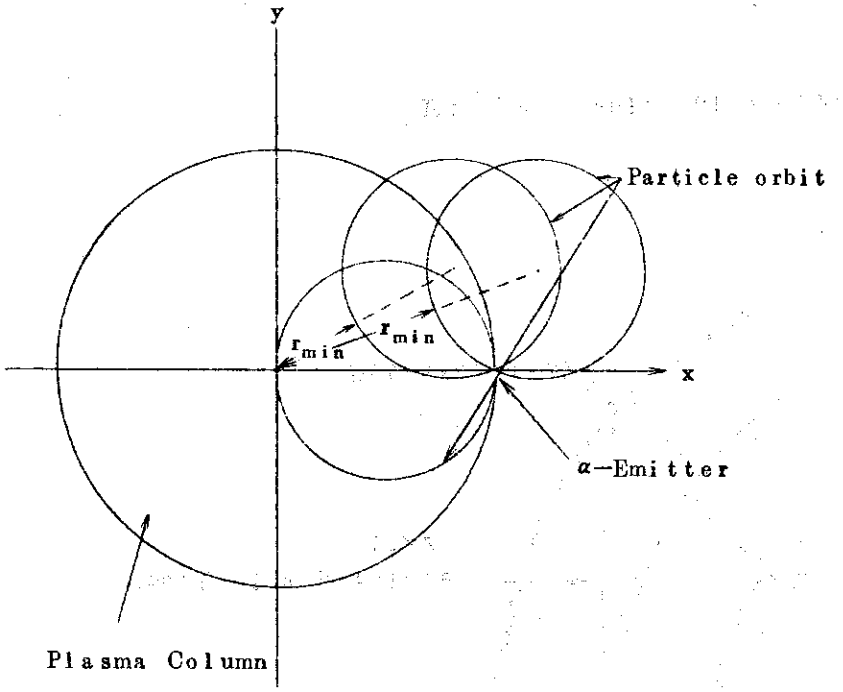

Fig. 9 Orbits of α-beams with various injection angles. Multiple α-beams are represented with the parameter d.

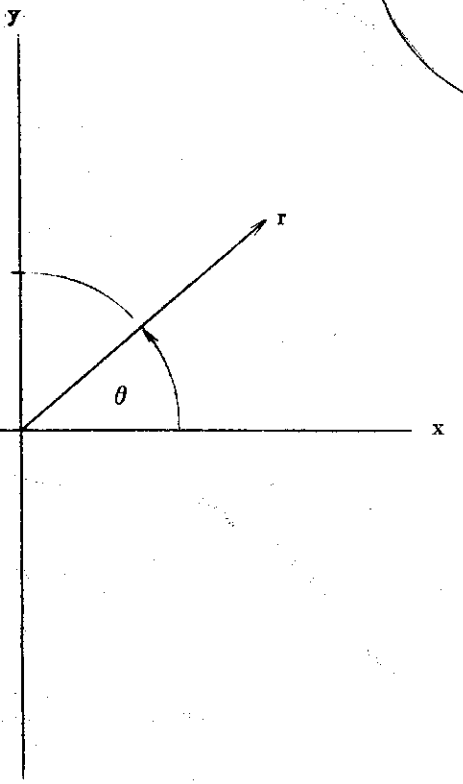

Fig. 10 Polar co-ordinates for calculating the deviations of the orbits with the parameter r_{min}.

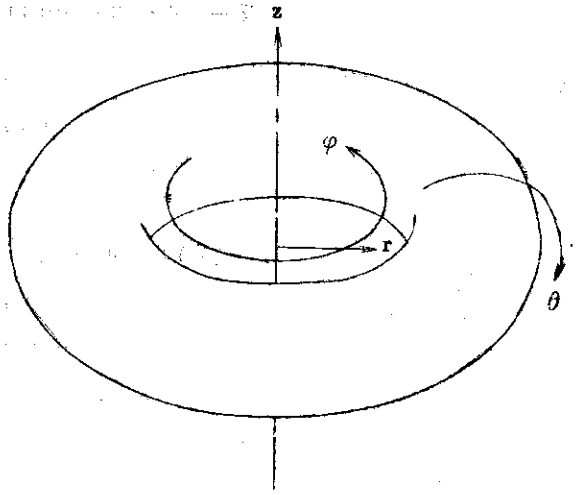

Fig. 11 Toroidal co-ordinates.

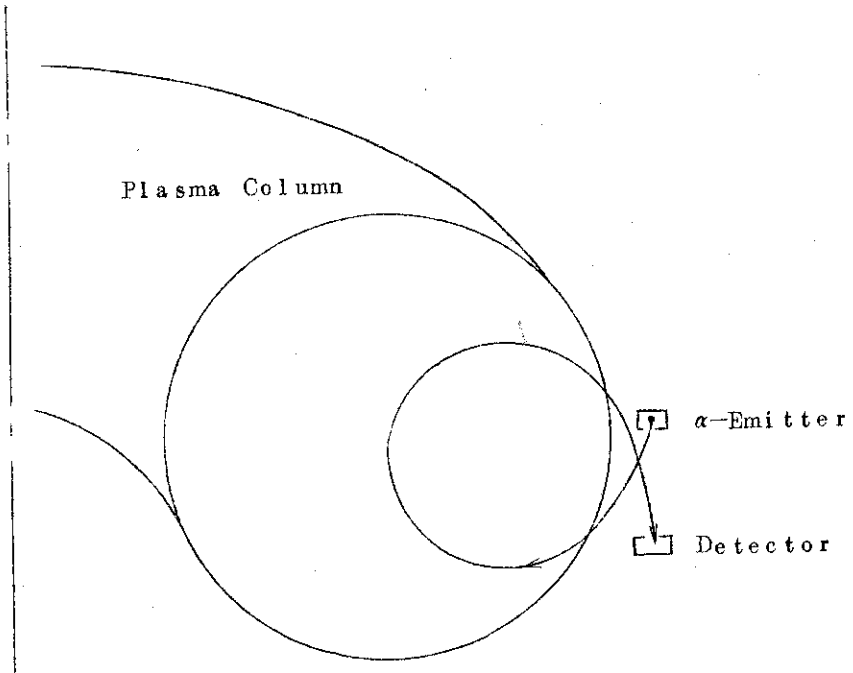

Fig. 12 Vertical Drift due to Toroidal Effect.

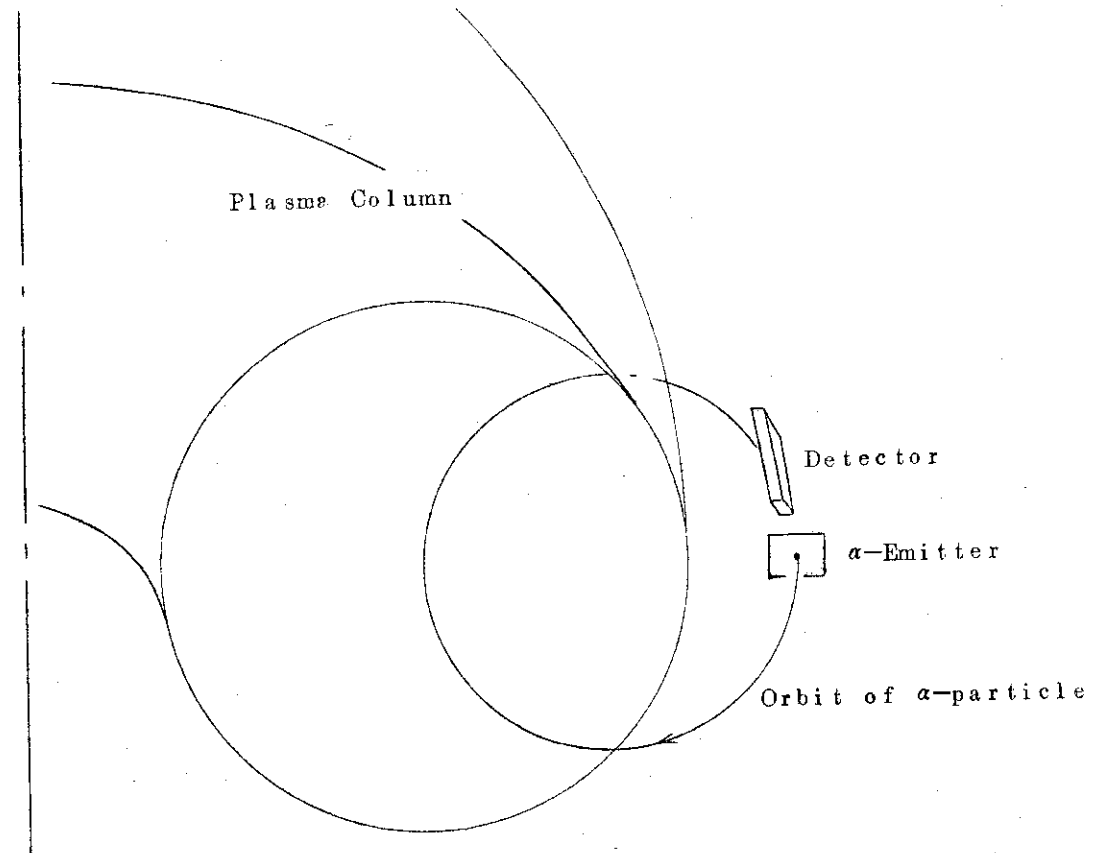

Fig. 13 Schematic figure of experimental arrangements of the α—emitter, slit system and detector.